Crystalline character of high-magnetic-field cusp states in quantum dots

Constantine Yannouleas and Uzi Landman
School of Physics, Georgia Institute of Technology, Atlanta, Georgia 30332-0430
(Dated: 31 December 2003; Revised 1 March 2004)

Conditional probability distributions from exact diagonalization are used to investigate the crystalline or liquid character of the downward cusp states in parabolic quantum dots (QD's) at high magnetic fields. These states are crystalline in character for fractional fillings covering both low and high values, unlike the liquid Jastrow-Laughlin wave functions, but in remarkable agreement with the rotating-Wigner-molecule ones [Phys. Rev. B **66**, 115315 (2002)]. The cusp states are precursors to the bulk fractional quantum Hall states (and not to the bulk Wigner crystal), since the collective rotation stabilizes the *rotating* Wigner molecule (formed in the QD) relative to the *static* one.

PACS numbers: 73.21.La; 71.45.Gm; 71.45.Lr

The excitation energy spectra of two-dimensional N-electron semiconductor quantum dots (QD's) in high magnetic fields (B) exhibit downward cusps [1, 2, 3, 4] at certain magic angular momenta, corresponding to states with enhanced stability. These cusp states have been long recognized [3, 4, 5, 6] as the finite-size precursors of fractional quantum Hall states in the bulk. In the literature of the fractional quantum Hall effect (FQHE), ever since the celebrated paper [7] by Laughlin in 1983, the cusp states have been considered to be the antithesis of the Wigner crystal and to be described accurately by liquid-like wave functions, such as the Jastrow-Laughlin [7, 8] (JL) and composite-fermion [9, 10] (CF) ones. This view, however, has been recently challenged [4] by the explicit derivation of trial wave functions for the cusp states that are associated with a rotating Wigner (or electron) molecule, RWM. As we discussed [4] earlier, the RWM wave functions, which are by construction *crystalline* in character, promise to provide a simpler, but yet improved and more consistent description of the properties of the cusp states, in particular for high angular momenta (L) [corresponding to low fractional fillings, since $\nu = N(N-1)/(2L)$].

Issues pertaining to the liquid or crystalline character of the cusp states are significant in both the fields of QD's and the FQHE. Since the many-body wave functions in the lowest Landau level (high B) obtained from exact diagonalization (EXD), the RWM, and the CF/JL have good angular momenta $L = L_0 = N(N-1)/2$ [6], their electron densities are *circularly* symmetric. Therefore investigation of the crystalline or liquid character of these states requires examination of the conditional probability distributions (CPD's, i.e., the fully anisotropic pair correlation functions). These calculations were performed here under high magnetic field conditions for QD's (in a disk geometry [11]) with $N = 6-9$ electrons, and for an extensive range of angular momenta. This allowed us to conclude that in all instances examined here (corresponding to $0.467 > \nu > 0.111$) the cusp states exhibit an unmistakably crystalline character, in contrast to the long held perception in the FQHE literature, with the RWM yielding superior agreement with the exact-diagonalization results. Furthermore, the RWM states are found to be energetically stabilized (i.e., exhibit gain in correlation energy) with respect to the corresponding *static* (symmetry-broken) Wigner molecules, from which the multideterminantal RWM wavefunctions are obtained through an angular-momentum projection [12].

The CPD's are defined by

$$P(\mathbf{r},\mathbf{r}_0) = \langle\Phi|\sum_{i\neq j}\delta(\mathbf{r}_i-\mathbf{r})\delta(\mathbf{r}_j-\mathbf{r}_0)|\Phi\rangle/\langle\Phi|\Phi\rangle, \quad (1)$$

where $\Phi(\mathbf{r}_1,\mathbf{r}_2,...,\mathbf{r}_N)$ denotes the many-body wave function under consideration. $P(\mathbf{r},\mathbf{r}_0)$ is proportional to the conditional probability of finding an electron at $\mathbf{r}$ under the condition that a second electron is located at $\mathbf{r}_0$. This quantity positions the observer on the moving (intrinsic) frame of reference specified by the collective rotations that are associated with the good angular momenta of the cusp states.

The CPD's for cusp states corresponding to a lower filling factor than $\nu = 1/5$, calculated for $N = 6$ electrons with $L = 135$ ($\nu = 1/9$, left column) and for $N = 6$ with $L = 105$ ($\nu = 1/7$, right column) are displayed in Fig. 1. Fig. 2 displays the CPD's for the cusp states with $N = 6$ electrons and $L = 75$ ($\nu = 1/5$, left column) and $N = 7$ and $L = 105$ ($\nu = 1/5$, right column). In both figures, the top row depicts the RWM case. The EXD case is given by the middle row, while the CF cases (which reduce to the JL wave functions for these fractions) are given by the bottom row.

There are three principal conclusions that can be drawn from an inspection of Figs. 1 and 2:

(I) The character of the EXD states is unmistakably crystalline with the EXD CPD's exhibiting a well developed molecular polygonal configuration [(1,5) for $N = 6$ and (1,6) for $N = 7$, with one electron at the center], in agreement with the explicitly crystalline RWM case.

(II) For all the examined instances (covering the fractional fillings 1/9, 1/7, and 1/5), the JL wave func-

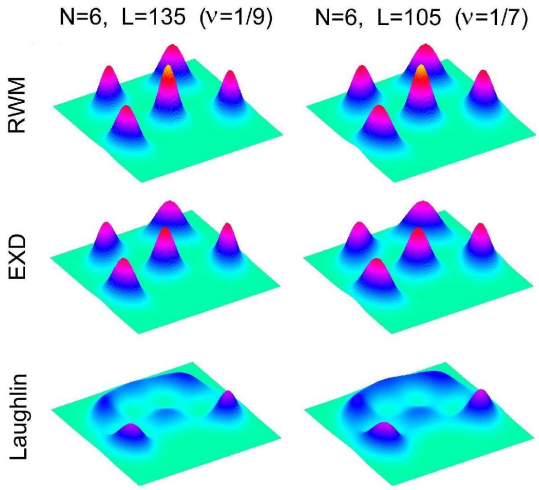

FIG. 1: Conditional probability distributions at high B for $N = 6$ electrons with $L = 135$ ($\nu = 1/9$, left column) and $L = 105$ ($\nu = 1/7$, right column). Top row: RWM case. Middle row: The case of exact diagonalization. Bottom row: The Jastrow-Laughlin case. It is apparent that the exact diagonalization and RWM wave functions have a pronounced crystalline character, corresponding to the (1,5) polygonal configuration of the rotating Wigner molecule. In contrast, the Jastrow-Laughlin wave functions fail to capture this crystalline character, exhibiting a rather "liquid" character. The observation point (identified by the missing electron hump) was placed at the maximum of the outer ring of the radial electron density [4] of the EXD wave function, namely at $r_0 = 7.318 l_B$ for $L = 135$ and $r_0 = 6.442 l_B$ for $L = 105$. The EXD Coulomb interaction energies (lowest Landau level) are 1.6305 and 1.8533 $e^2/\kappa l_B$ for $L = 135$ and $L = 105$, respectively. Here, $l_B = (\hbar c/eB)^{1/2}$. The errors relative to the corresponding EXD energies and the overlaps of the trial functions with the EXD ones are: (I) For $L = 135$, RWM: 0.34%, 0.860; JL: 0.50%, 0.665. (II) For $L = 105$, RWM: 0.48%, 0.850; JL: 0.46%, 0.710.

tions fail to capture the intrinsic crystallinity of the EXD states. In contrast, they represent "liquid" states in agreement with an analysis that goes back to the original papers [7, 8] by Laughlin. In particular, Ref. [8] investigated the character of the JL states through the use of a pair correlation function [usually denoted by $g(R)$] that determines the probability of finding another electron at the absolute relative distance $R = |\mathbf{r} - \mathbf{r}_0|$ from the observation point $\mathbf{r}_0$. Our anisotropic CPD of Eq. (1) is of course more general (and more difficult to calculate) than the $g(R)$ function of Ref. [8]. However, both our $P(\mathbf{r}, \mathbf{r}_0)$ (for $N = 6$ and $N = 7$ electrons) and the $g(R)$ (for $N = 1000$ electrons, and for $\nu = 1/3$ and $\nu = 1/5$) in Ref. [8] reveal a similar characteristic liquid-like short-range-order behavior for the JL states, eloquently described in Ref. [8] (see p. 249 and p. 251). Indeed, we remark that only the first-neighbor electrons on the outer rings can be distinguished as separate localized electrons in our CPD plots of the JL functions [see Fig. 1 and Fig. 2].

(III) The pronounced crystallinity of the EXD states at the rather high $\nu = 1/5$ value (see Fig. 2) does not support the long held expectation [7, 8, 13] (based on extrapolations of the JL wave functions to the bulk and comparisons with the static bulk Wigner crystal) that a liquid-to-crystal phase transition may take place only at the lower fillings with $\nu \leq 1/7$.

Following the conclusion that the crystalline character of the cusp states in QD's is already well developed for fractional fillings with the unexpected high value of $\nu = 1/5$, a natural question arises concerning the presence or absence of crystallinity in cusp states corresponding to higher fractional fillings, i.e., states with $1/5 < \nu < 1/3$, and even with $1/3 < \nu < 1$. To answer this question, we show in Fig. 3 the CPD's for the RWM (left column) and EXD (right column) wave functions for the case of $N = 7$ and $L = 45$ ($1/3 < \nu = 7/15 < 1$), of $N = 8$ and $L = 91$ ($1/5 < \nu = 4/13 < 1/3$), and of $N = 9$ and $L = 101$ ($1/3 < \nu = 36/101 < 1$). Unlike the

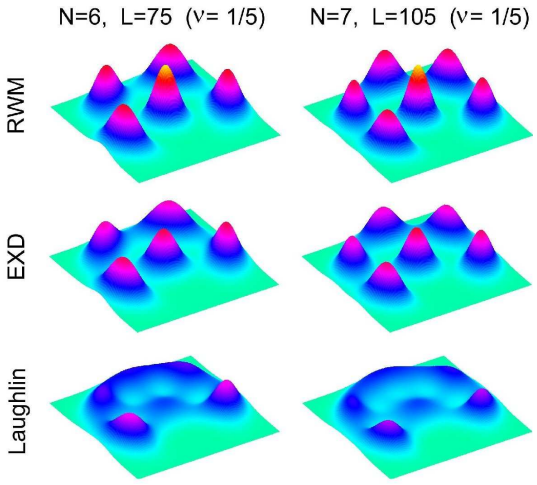

FIG. 2: Conditional probability distributions at high B for $N = 6$ electrons and $L = 75$ ($\nu = 1/5$, left column) and for $N = 7$ electrons and $L = 105$ (again $\nu = 1/5$, right column). Top row: RWM case. Middle row: The case of exact diagonalization. Bottom row: The Jastrow-Laughlin case. The exact diagonalization and RWM wave functions have a pronounced crystalline character, corresponding to the (1,5) polygonal configuration of the RWM for $N = 6$, and to the (1,6) polygonal configuration for $N = 7$. In contrast, the Jastrow-Laughlin wave functions exhibit a characteristic liquid profile that depends smoothly on the number N of electrons. The observation point is located at $r_0 = 5.431 l_B$ for $N = 6$ and $L = 75$ and $r_0 = 5.883 l_B$ for $N = 7$ and $L = 105$. The EXD Coulomb interaction energies (lowest Landau level) are 2.2018 and 2.9144 $e^2/\kappa l_B$ for $N = 6, L = 75$ and $N = 7, L = 105$, respectively. The errors relative to the corresponding EXD energies and the overlaps of the trial functions with the EXD ones are: (I) For $N = 6, L = 75$, RWM: 0.85%, 0.817; JL: 0.32%, 0.837. (II) For $N = 7, L = 105$, RWM: 0.59%, 0.842; JL: 0.55%, 0.754.

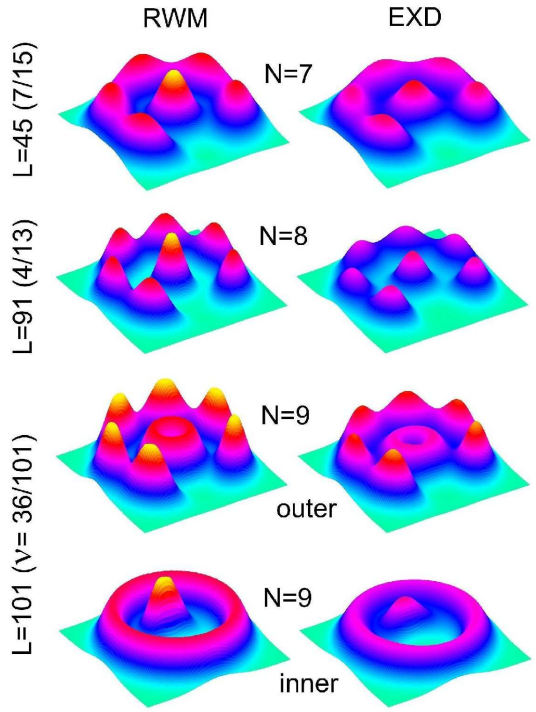

FIG. 3: Additional CPD's at high B. RWM results: Left column. Results from exact diagonalization are depicted on the right column. Top row: $N = 7$ electrons and $L = 45$ $(1/3 < \nu = 7/15 = 0.467 < 1)$ Middle row: $N = 8$ electrons and $L = 91$ $(1/5 < \nu = 4/13 = 0.308 < 1/3)$. Two bottom rows: $N = 9$ electrons and $L = 101$ $(1/3 < \nu = 36/101 = 0.356 < 1$, see text for explanation). Even for these low magic angular momenta (high fractional fillings), both the exact-diagonalization and RWM wave functions have a pronounced crystalline character [corresponding to the (1,6), (1,7), and (2,7) polygonal configuration of the RWM for $N = 7$, 8, and 9 electrons]. The observation point is located at $r_0 = 3.776 l_B$ for $N = 7, L = 45$, $r_0 = 5.105 l_B$ for $N = 8, L = 91$, and $r_0 = 5.218 l_B$ (outer) and $r_0 = 1.662 l_B$ (inner) for $N = 9, L = 101$.

long held perceptions in the FQHE literature (which were reasserted in a recent manuscript [14]), the CPD's in Fig. 3 demonstrate that the character of the cusp states with high fractional fillings is not necessarily "liquid-like". Instead, these high-ν cusp states can exhibit a well developed crystallinity associated with the (1,6), (1,7), and (2,7) polygonal configurations of the RWM, appropriate for $N = 7$, 8, and 9 electrons, respectively. Similar results were also found for the case of $N = 6$ electrons. Note that the case of $N = 9$ represents the smallest number of electrons with a non-trivial concentric-ring arrangement, i.e., the inner ring has more than one electrons. As the two CPD's [reflecting the choice of taking the observation point ($\mathbf{r}_0$ in Eq. (1)) on the outer or the inner ring] for $N = 9$ reveal, the polygonal electron rings rotate independently of each other. Thus, e.g., to an observer located on the inner ring, the outer ring will appear as uniform.

Our two-step method for deriving the RWM wave functions is anchored in the distinction [15] between a *static* and a *rotating* Wigner molecule, with the collective rotation stabilizing the latter relative to the former. Further elaboration on this point requires generation of global ground states out of the cusp states, achieved through inclusion [5, 15] of an external parabolic confinement (of frequency ω_0). In the two-step method, the static WM is first described by an unrestricted Hartree-Fock (UHF) determinant that violates the circular symmetry [16]. Subsequently, the collective rotation of the WM is described by a post-Hartree-Fock step of restoration of the broken circular symmetry via projection techniques [12]. We note that, in the limit $N \to \infty$, the static WM of the UHF develops to the bulk Wigner crystal [17] and its more sophisticated variants [13].

In general, the localized broken symmetry orbitals of the HF determinant are determined numerically via a selfconsistent solution of the UHF equations [16]. Since we focus here on the case of high B, we can approximate the UHF orbitals (first step of our procedure) by (parameter free) displaced Gaussian functions; namely, for an electron localized at Z_j, we use the orbital

$$u(z, Z_j) = \frac{1}{\sqrt{\pi}\lambda} \exp\left(-\frac{|z - Z_j|^2}{2\lambda^2} - i\varphi(z, Z_j; B)\right), \quad (2)$$

with $z = x + iy$, $Z_j = X_j + iY_j$, and $\lambda = \sqrt{\hbar/m^*\Omega}$; $\Omega = \sqrt{\omega_0^2 + \omega_c^2/4}$, where $\omega_c = eB/(m^*c)$ is the cyclotron frequency. The phase guarantees gauge invariance in the presence of a perpendicular magnetic field and is given in the symmetric gauge by $\varphi(z, Z_j; B) = (xY_j - yX_j)/2l_B^2$, with $l_B = \sqrt{\hbar c/eB}$. We only consider the case of fully polarized electrons, which is appropriate at high B.

We take the Z_j's to coincide with the equilibrium positions (forming nested regular polygons) of N classical point charges inside an external parabolic confinement of frequency ω_0, and proceed to construct the UHF determinant $\Psi^{\rm UHF}[z]$ out of the orbitals $u(z_i, Z_i)$'s, $i = 1, ..., N$. Correlated many-body states with good total angular momenta L can be extracted [12] from the UHF determinant using projection operators. We stress that while the initial trial wave function of the UHF equations consists of a single determinant, the projected wave function is a linear superposition of many determinants. The projected energy, corresponding to the symmetry-restored state with angular momentum L, is given by [12]

$$E_{\rm PRJ}(L) = \int_0^{2\pi} h(\gamma) e^{i\gamma L} d\gamma \Big/ \int_0^{2\pi} n(\gamma) e^{i\gamma L} d\gamma, \quad (3)$$

with $h(\gamma) = \langle \Psi^{\rm UHF}(0)|H|\Psi^{\rm UHF}(\gamma)\rangle$ and $n(\gamma) = \langle \Psi^{\rm UHF}(0)|\Psi^{\rm UHF}(\gamma)\rangle$, where $\Psi^{\rm UHF}(\gamma)$ is the original UHF determinant rotated by an azimuthal angle γ and H is the many body Hamiltonian (comprised [12] of the kinetic energy with a vector potential for the magnetic

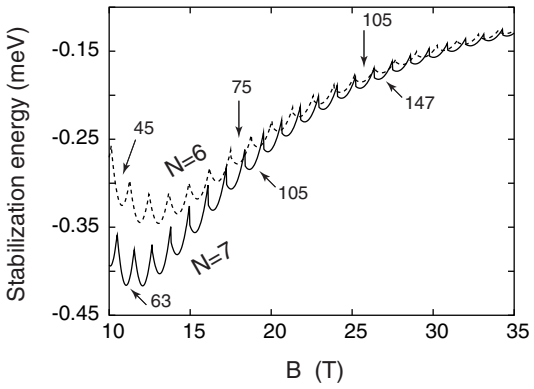

FIG. 4: Stabilization energies $\Delta E_{\rm gs}^{\rm gain} = E_{\rm PRJ}^{\rm gs} - E_{\rm UHF}$ for $N = 6$ (dashed curve) and $N = 7$ (solid curve) fully polarized electrons in a parabolic QD as a function of B. The troughs associated with the major fractional fillings (1/3, 1/5, and 1/7) and the corresponding ground-state angular momenta are indicated with arrows. We have extended the calculations up to $B = 120$ T (not shown), and verified that $\Delta E_{\rm gs}^{\rm gain}$ remains negative while its absolute value vanishes as $B \to \infty$. The choice of parameters is: $\hbar\omega_0 = 3$ meV (parabolic confinment), $m^* = 0.067 m_e$ (electron effective mass), and $\kappa = 12.9$ (dielectric constant).

field, an external confinement, the Coulomb interelectron repulsion, and the Zeeman term). The UHF energies are simply given by $E_{\rm UHF} = h(0)/n(0)$.

We note that, unlike the UHF ground state (describing a static Wigner molecule) which has no good angular momentum, the ground states of the RWM exhibit good angular momenta (labeled as $L_{\rm gs}$) that coincide with magic ones [we denote the ground-state energy of the RWM as $E_{\rm PRJ}^{\rm gs} \equiv E_{\rm PRJ}(L_{\rm gs})$].

The stabilization of the *rotating* WM relative to the *static* one [namely the fact that $E_{\rm PRJ}^{\rm gs} < E_{\rm UHF}$, see Fig. 4] is a purely quantum effect. This energy gain demonstrated here for $N = 6$ and 7 electrons, is in fact a general property of states projected out of trial functions with broken symmetry. This is due to a theorem [18] stating that at least one of the projected states (i.e., the ground state) has an energy lower than that of the original broken-symmetry trial function (e.g., the UHF determinant considered above).

While our focus here is on the behavior of trial and exact wave functions in (finite) QD's in high magnetic fields, it is natural to inquire about the implications of our findings to FQHE systems in the thermodynamic limit. We recall that appropriate trial wave functions for clean FQHE systems must possess a good angular momentum $L \geq L_0$, a property shared by both the CF/JL and RWM functions. We also recall the previous finding that for small fractional fillings ν the static Wigner crystal (which is a broken-symmetry state with no good angular momentum) is energetically favored [7, 8, 10, 13] compared to the (liquid-like) CF/JL wave function. In contrast, the RWM wave functions remain lower in energy than the corresponding static crystalline state for *all values* of N and ν, even in the thermodynamic limit. This is due to the fact that the aforementioned "energy-gain" theorem [18] applies for any number of electrons N and for all values of the magnetic field B [19].

Since the rotating Wigner crystal carries a current, while the static crystal is insulating, we may conjecture that a transition at lower fractional fillings from a FQHE conducting state to an insulating Wigner crystal cannot occur *spontaneously* for clean systems. Therefore, it should be possible to observe (see, e.g., Ref. [20]) FQHE behavior at all fractional fillings in a clean system. In practice, however, impurities and defects, may pin the RWM, so that one of the main challenges for FQHE observation at such low fillings relates to fabrication of high mobility samples [21, 22].

In summary, we have carried out the first systematic investigations (for $6 \leq N \leq 9$) of cusp states in parabolic quantum dots at high magnetic fields. Our anisotropic conditional probability distributions from exact diagonalization show that these states are crystalline in character for both low and high fractional fillings, unlike the liquid-like Jastrow-Laughlin [7, 8] wave functions, but in remarkable agreement with the recently proposed rotating-Wigner-molecule [4] ones. The cusp states of finite-N parabolic QD's are precursors to the bulk fractional quantum Hall states (and not to the bulk Wigner crystal) due to the collective rotation, which stabilizes the *rotating* Wigner molecule (having a good angular momentum) relative to the *static* one (that exhibits broken symmetry).

We thank M. Pustilnik for comments on the manuscript. This research is supported by the U.S. D.O.E. (Grant No. FG05-86ER45234).

[1] R.B. Laughlin, Phys. Rev. B **27**, 3383 (1983).
[2] P.A. Maksym and T. Chakraborty, Phys. Rev. Lett. **65**, 108 (1990).
[3] J.K. Jain and T. Kawamura, Europhys. Lett. **29**, 321 (1995).
[4] C. Yannouleas and U. Landman, Phys. Rev. B **68**, 035326 (2003); **66**, 115315 (2002).
[5] S.R.E. Yang, A.H. MacDonald, and M.D. Johnson, Phys. Rev. Lett. **71**, 3194 (1993).
[6] A.L. Jacak, P. Hawrylak, and A. Wojs, *Quantum Dots* (Springer, Berlin, 1998), in particular Ch. 4.5.
[7] R.B. Laughlin, Phys. Rev. Lett. **50**, 1395 (1983).
[8] R.B. Laughlin, in *The Quantum Hall Effect*, Edited by R.E. Prange and S.M. Girvin (Springer, New York, 1987) p. 233
[9] J.K. Jain, Phys. Rev. B **41**, 7653 (1990).
[10] S.S. Mandal, M.R. Peterson, and J.K. Jain, Phys. Rev. Lett. **90**, 106403 (2003).
[11] The results in Figs. 1-3 were obtained without consider-

ation of a confinement, and they are not influenced (high B) by inclusion of a parabolic confinement [3, 5, 15]. For the influence of the confinement on the energies, see Refs. [3, 5, 15].

[12] C. Yannouleas and U. Landman, J. Phys.: Condens. Matter **14**, L591 (2002); Phys. Rev. B **68**, 035325 (2003), and references therein.

[13] P.K. Lam and S.M. Girvin, Phys. Rev. B **30**, 473 (1984).

[14] G.S. Jeon, C.-C. Chang, and J.K. Jain, cond-mat/0310287.

[15] C. Yannouleas and U. Landman, cond-mat/0311480.

[16] C. Yannouleas and U. Landman, Phys. Rev. Lett. **82**, 5325 (1999); Phys. Rev. B **61**, 15 895 (2000).

[17] D.J. Yoshioka and P.A. Lee, Phys. Rev. B **27**, 4986 (1983).

[18] See sect. 3 in P.-O. Löwdin, Rev. Mod. Phys. **34**, 520 (1962).

[19] We remark that, at present, computational difficulties prohibit a straightforward extrapolation of energy to the thermodynamic limit as a function of N and ν. This is the case especially for the disk geometry used here, which is advantageous for studies of crystalline structures, compared to the computationally easier spherical geometry.

[20] W. Pan *et al.*, Phys. Rev. Lett. **88**, 176802 (2002).

[21] L. Pfeiffer and K.W. West, Physica E **20**, 57 (2003).

[22] We remark, however, that the stabilization energy diminishes as $B \to \infty$ (see Fig. 4), and as a result the impurities become more efficient in pinning the WM for the lower fractional fillings (i.e., higher angular momenta).